The Thomson problem for N = 10

Peter Graham
https://orcid.org/0009-0007-8493-1505

First published October 22, 2026; this version November 20, 2026 (v12)
Zenodo archive (Lean development in `lean`, checkers in `checks`):
https://doi.org/10.5281/zenodo.23552641

hexagon:2611.00836v1

Abstract

For ten distinct points on the unit sphere, we prove that the bicapped square antiprism uniquely minimizes Coulomb energy, up to orthogonal transformations and relabeling. We build on the Lean proof directed by Aravind Karthigeyan of the tricapped trigonal prism's nine-point optimality and uniqueness. We use the three-point positivity method of Bachoc and Vallentin and of Cohn and Woo. A three-point semidefinite bound confines every competitor of no greater energy to short intervals around the candidate's inner products. Gram-determinant tests determine their assignment to pairs; orthogonal alignment and a quantitative local energy inequality then force congruence. The candidate's height is the unique critical point in a rational interval. We formalize the argument in Lean.

This work has not yet been reviewed by experts. The proofs, the Lean formalization, the certificate checkers and the text were produced by AI models, working under the author's direction.

1 Introduction

For an injective map $x : \{0, \dots, 9\} \to S^2 \subset \mathbb{R}^3$, put

$$\mathcal{E}(x) = \sum_{0 \le i < j \le 9} \frac{1}{\|x_i - x_j\|}.$$

We call two configurations congruent when one is obtained from the other by an element of $O(3)$ and a permutation of the ten indices; reflections are allowed.

The candidate $p(h)$ is the bicapped square antiprism: two poles and two squares at opposite heights, rotated by $\pi/4$ (Figure 1); Section 2.1 gives its coordinates. The energy of this family is $F(h) = \mathcal{E}(p(h))$, with the explicit expression in (5). Write $S(h) = F'(h)$. Let $[a, b]$ be the exact rational interval in Appendix D.1, and define h_* by $S(h_*) = 0$ and $h_* \in [a, b]$; numerically, $h_* \approx 0.4226874$.

Theorem 1. *The parameter h_* exists and is unique in $[a, b]$. The configuration $p = p(h_*)$ consists of ten distinct points on S^2. For every injective $x : \{0, \dots, 9\} \to S^2$,*

$$\mathcal{E}(p) \le \mathcal{E}(x), \qquad \mathcal{E}(x) = \mathcal{E}(p) \iff \exists Q \in O(3),\ \exists \sigma \in S_{10},\ x_i = Q p_{\sigma(i)} \text{ for all } i.$$

Thomson wrote *On the structure of the atom* [1, p. 237]. Our formalization reuses most of the nine-point Lean proof of optimality and uniqueness directed by Karthigeyan [2]. New three-point,

classification and Hessian bounds prove the theorem. The main difficulty is making the three-point bound accurate enough to force the candidate's seven inner-product intervals.

Föppl's list of stable arrangements includes $10 = 1 + 4 + 4 + 1$ [7, p. 190]. Yudin's simplex and cross-polytope optima and Andreev's icosahedron are credited by Cohn and Kumar [9, Section 1]; see also [4, 8]. Cohn and Kumar's universal-optimality result is Theorem 1.2 and Table 1 of [9]. Schwartz proved the five-point case [10, Theorem 1.1]. For numerical data, see Erber and Hockney [11, Fermilab preprint, Table 1] and Wales and Ulker [12].

Bachoc and Vallentin [5, Section 1] credit the linear programming method to Delsarte, Goethals and Seidel [3]. Cohn and Woo [6, Section 1.1] credit its first energy-minimization application to Yudin [4]. Our three-point bound uses Bachoc and Vallentin [5, Corollary 3.5] and Cohn and Woo [6, Theorem 5].

Tran proves optimality and uniqueness of the pentagonal bipyramid for seven charges [14]. Kryvonos, Liehr and Taylor prove optimality and uniqueness of the eight-point square antiprism [15, Theorem 1.1]. Tooby-Smith and Zughaid give a separate, ongoing Lean development for eight charges [16]. Zarco gives exact three-point certificates for the five-point Riesz energies with exponents one through six and Lean developments for exponents one and two [17]. Zarco's seven-point project treats uniqueness of the pentagonal bipyramid for logarithmic and inverse-square energies; its Coulomb argument uses Tran's local lemma [18]. Concurrent ten-point Lean work by `saberwatchmanga` (formerly `terry2418`) includes the October 7 local-minimum proof in the full space of ten unit-sphere points [13, 19]. The cutoff 32.717 also appears in [20], which proves that energy at most this value forces a pair farther apart than 1.935.

Jingxing Huang also reports a separate nine-point Lean proof candidate, with conditional independent Python checking [24, README and manuscript abstract]. Xie's preprint, posted on November 2, 2026, eleven days after the first version of this work (October 22, 2026) [23], independently proves optimality and uniqueness for nine and ten charges [22, Theorem 1.1], using three-point energy bounds, Gram classification and a Hessian bound with exact and interval arithmetic.

This work is checked in Lean from the definitions (Section 3).

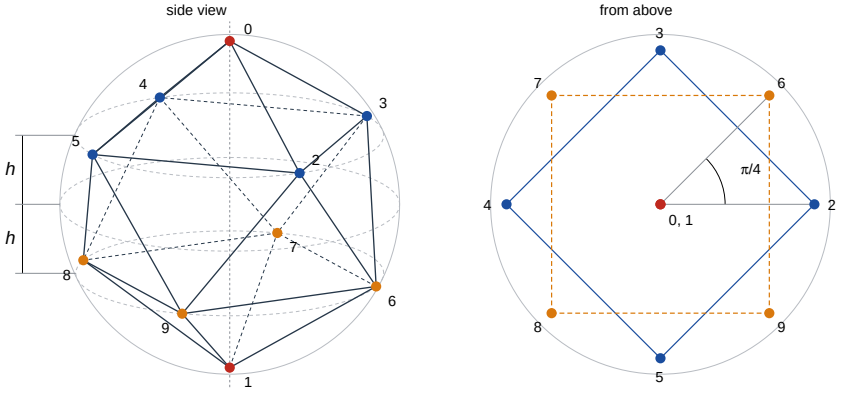

Figure 1: The bicapped square antiprism, viewed from the side and from above. The labels identify the points in Section 2.1.

2 Proof of the main theorem

Optimizing its height alone would not exclude asymmetric competitors. The three-point bound forces pairwise inner products into short intervals; Gram-determinant tests determine their assignment to pairs, and orthogonal alignment brings the competitor into the region where a positive second variation and an explicit remainder bound apply.

2.1 The bicapped square antiprism

We define the candidate and isolate its height. For $0 < h < 1$, write $r = \sqrt{1-h^2}$ and $q = r/\sqrt{2}$. Define $p(h)$ by

$$\begin{aligned} &p_0 = (0,0,1), && p_1 = (0,0,-1), \\ &p_2 = (r,0,h), && p_3 = (0,r,h), && p_4 = (-r,0,h), && p_5 = (0,-r,h), \\ &p_6 = (q,q,-h), && p_7 = (-q,q,-h), && p_8 = (-q,-q,-h), && p_9 = (q,-q,-h). \end{aligned}$$

These coordinates are preserved by rotation through $\pi/4$ about the polar axis followed by reflection in the equatorial plane, and by reflection in the vertical plane through p_2 and the poles. The 16-element group generated by these maps is conventionally denoted D_{4d}.

The derivative S is continuous and strictly increasing on $[a,b]$, and its endpoint signs satisfy $S(a) < 0 < S(b)$. The intermediate value theorem and strict monotonicity therefore give a unique zero in this interval. Define h_* by $S(h_*) = 0$ and $h_* \in [a,b]$. An admissible configuration is an injective map to S^2. The coordinate verification is in Appendix A.

The seven distinct inner products of the candidate are

$$-1, \quad h_*, \quad -h_*, \quad h_*^2, \quad 2h_*^2 - 1, \quad \frac{1-h_*^2}{\sqrt{2}} - h_*^2, \quad -\frac{1-h_*^2}{\sqrt{2}} - h_*^2.$$

2.2 From energy bounds to a common interval pattern

We now show that every admissible competitor of energy at most the candidate's has nearly the same matrix of pairwise inner products, after relabeling. Let $f(t) = (2-2t)^{-1/2}$. For unit vectors, the pair energy is $f(\langle x_i, x_j\rangle)$. Throughout this section, $p = p(h_*)$ and x is an arbitrary admissible configuration satisfying $\mathcal{E}(x) \le \mathcal{E}(p)$.

We bound the energy lost by replacing the pair potential with a polynomial; this loss will force every pair into one of seven short intervals.

Separation of points. For a competitor of energy at most $\mathcal{E}(p)$, a two-point bound first gives $\langle x_i, x_j\rangle < 13/20$ for distinct indices. The polynomial verification is given in Appendix D.2.

Three-point bound. The next bound uses a fixed rational polynomial and a finite set of rational matrices; together these data form the *three-point certificate*. Define $m(t) = \sum_{j=0}^{16} c_j t^j - 2^{-130}$, where the coefficients c_j are the rational data in the supplement [21]. The downward shift ensures that m lies below f throughout $[-1, 13/20]$. Let U be the fixed rational upper bound in the certificate.

For three unit vectors x_i, x_j, x_k, use the argument convention $u = \langle x_i, x_j\rangle$, $v = \langle x_i, x_k\rangle$ and $t = \langle x_j, x_k\rangle$. The matrices specify two polynomials K and W. The data and kernel polynomials are defined in Appendices D.3 and D.4. Define the residual polynomial $\mathcal{R}$ by

$$\frac{m(u)+m(v)+m(t)}{3} - \frac{U - 45\cdot 2^{-130}}{45} = K(u,v,t) + W(u,v,t) + \mathcal{R}(u,v,t).$$

Here $\|\mathcal{R}\|_1$ is the sum of the absolute values of the residual's rational coefficients.

First, the sum of K over all ordered triples of distinct indices is nonnegative for every configuration of ten unit vectors.

Define polynomials $C_n(\alpha, \beta)$ by

$$C_0 = 1, \qquad C_1 = \alpha, \qquad C_{n+2} = 2\alpha C_{n+1} - \beta C_n, \qquad T_k(u, v, t) = C_k(t - uv, (1 - u^2)(1 - v^2)).$$

Here u and v are the inner products with the first, distinguished point, and t is the inner product of the other two points. Fixing that first point and projecting the others onto its perpendicular plane identifies the projected vectors with complex numbers. The recurrence expresses real parts of their powers. Therefore the quadratic sums of T_k, with weights given by products of real point weights, are squared absolute values of complex sums and are nonnegative. This is the spherical three-point positivity used in the proof.

For exact prior statements see Bachoc–Vallentin [5, Corollary 3.5] and Cohn–Woo [6, Theorem 5]. The repeated-index corrections are defined in Appendix D.3. Second, W is a sum of weighted polynomial squares, and is nonnegative on the Gram domain defined by $u, v, t \in [-1, 13/20]$, $1 + 2uvt - u^2 - v^2 - t^2 \geq 0$. The six weights are listed in Appendix D.4. The residual estimate is given there as well. Every residual monomial has absolute value at most one on this domain, so this coefficient sum bounds the residual pointwise. Put $L = 45(2^{-130} + \|\mathcal{R}\|_1)$.

Lemma 1 (Certified energy bound)**.** *For the fixed polynomial m and constants U, L just specified, every configuration of ten unit vectors with $\langle x_i, x_j \rangle \leq 13/20$ for all $i \neq j$ satisfies*

$$\mathcal{E}(p) \leq U \leq 32717/1000, \qquad U - L \leq \sum_{i<j} m(\langle x_i, x_j \rangle), \qquad L < 10^{-30}.$$

Averaging the residual identity over the $10 \cdot 9 \cdot 8$ ordered triples of distinct indices turns its pair term into $\sum_{i<j} m(\langle x_i, x_j \rangle)/45$. This is because each of the 45 unordered pairs occurs equally often in the three positions. The polynomial shift 2^{-130} is included in m, so the reference constant is $(U - 45 \cdot 2^{-130})/45$. Bounding the averaged residual by $\|\mathcal{R}\|_1$ and multiplying by 45 gives $U - L$.

For each pair, call the nonnegative difference between its true energy and its polynomial lower bound its *slack*. Their total is at most L, because the energy is at most that of the candidate:

$$\sum_{i<j} (f - m)(\langle x_i, x_j \rangle) = \mathcal{E}(x) - \sum_{i<j} m(\langle x_i, x_j \rangle) \leq \mathcal{E}(p) - (U - L) \leq L.$$

Localization of inner products. A *window* is an open interval of radius $\delta = 10^{-10}$ centered at one of the seven candidate inner products in Section 2.1. The slack satisfies $f(t) - m(t) \geq 10^{-30}$ for every $t \in [-1, 13/20]$ outside all seven windows. Since $L < 10^{-30}$, even one pair outside the windows would exceed the total available slack. Every pair therefore belongs to a window.

2.2.1 Classification of inner-product assignments

We now classify which assignments of these seven windows to the pairs can arise from ten unit vectors in three dimensions. Number the seven candidate inner products by the colors zero through six, as in the table in Appendix B. Assign a color to each pair according to the window containing its inner product. The windows are disjoint, so each pair has just one color.

An *anchor triple* consists of three points whose three-by-three Gram matrix has determinant greater than $1/100000$. Such a triple is linearly independent. For each sorted triple of pair colors, evaluate the three-by-three Gram determinant over rational outer enclosures of the three windows.

The resulting *determinant interval* contains every determinant that those colors can realize. An anchor *type* is a sorted triple of pair colors. A type is *eligible* when this interval's upper endpoint is greater than the threshold; every actual anchor triple has an eligible type.

The determinant intervals show that a triangle with determinant at most the threshold can have only a color permutation of $(0, 1, 2)$, $(1, 1, 4)$ or $(2, 2, 4)$. Each such triangle has exactly one edge of color zero or four. If every triangle among the five configuration points with indices zero through four had one of these types, counting these marked edges over the ten triangles would give ten. But each edge belongs to three triangles, so the same count must be divisible by three. This contradiction supplies an anchor triple. Each of the remaining seven points determines a *node*: the three colors of its pairs with the three anchor points. The four-by-four Gram determinant of this point and the anchor points vanishes because four vectors lie in three dimensions; interval evaluation removes nodes for which this is impossible.

For two remaining points, form a four-by-four matrix with rows indexed by the three anchor points followed by the first point, and columns indexed by the same three anchor points followed by the second point. Each entry is the inner product of its row-index and column-index vectors. This matrix has rank at most three, so its determinant vanishes. Two nodes are *compatible* with a proposed color between them when interval evaluation of this determinant contains zero. The nodes specify the windows for inner products with the anchor points, and the proposed color specifies the window for the one remaining entry.

Two nodes are adjacent when at least one color survives the compatibility condition, retaining the list of all surviving colors on that edge. A *clique* is a set of seven nodes with an edge between every two. The seven remaining points of an actual configuration give such a clique. They give distinct nodes because the compatibility condition excludes all seven colors when the two node indices are equal; that test still allows the two points' inner products with the anchors to vary independently within the same windows.

The enumeration checks every clique in every eligible anchor type. For each clique, its witness is a bijection from the three anchor points and seven nodes to the candidate's ten indices. The witness preserves the anchor and node colors and checks *every surviving color* on each clique edge against the candidate color. Thus no separate choice of edge colors is needed: all colors that an actual configuration could use are forced to agree with the same candidate labeling.

Classification. The finite classification proves that there exists a permutation τ for which

$$|\langle x_{\tau(i)}, x_{\tau(j)}\rangle - \langle p_i, p_j\rangle| \le \delta \quad \text{for all } i, j. \tag{1}$$

Thus each pair has been assigned the same window as the corresponding candidate pair. The permutation τ labels the competitor by the candidate indices.

2.3 Alignment and strict local minimality

This section proves that a competitor of no greater energy satisfying (1) is congruent to the candidate. We first align it with the candidate and then show that any remaining displacement raises energy.

2.3.1 From inner products to point displacements

Among orthogonal maps, choose Q minimizing the sum of squared displacements from p, and put

$$y_i = Q x_{\tau(i)}, \qquad \eta_i = y_i - p_i, \qquad \rho^2 = \sum_i \|\eta_i\|^2.$$

Write $\eta \in \mathbb{R}^{30}$ for the concatenation of the ten displacement vectors η_i. The quantity ρ is their total displacement. A quantitative Gram-stability argument turns (1) into an orthogonal alignment. It uses the candidate anchor points p_2, p_3, p_6: the absolute values of the inner products of pairs $(2,3)$, $(2,6)$ and $(3,6)$ are at most $19/100$, $41/100$ and $41/100$, respectively. The corresponding pairs of relabeled competitor anchor points consequently satisfy the absolute inner-product bounds $1/5, 5/12, 5/12$. In Gram–Schmidt, each residual is the component of an anchor point orthogonal to the span of the preceding anchor points. The lengths of the two residuals are at least $2/3$ and $1/2$. Thus the divisions used to recover coordinates from inner products have denominators bounded away from zero.

In the resulting orthonormal frames, the coordinate differences for each point are at most δ, 22δ and 646δ, respectively. These scalar estimates follow by applying the product, square-root and quotient difference bounds to the Gram–Schmidt formulas; they are proved by scalar perturbation estimates with rational constants. Relaxing each to 650δ and summing the 30 coordinate squares gives $\rho^2 \le 30(650\delta)^2 \le (10000\delta)^2$ for the constructed alignment. Minimality transfers this bound to the minimizing alignment. Thus

$$\rho \le 10000\delta = 10^{-6}.$$

Minimality of this orthogonal Procrustes alignment—least squares over orthogonal maps—also gives the skew conditions below. Here k, l index the three coordinates, and $\eta_{i,k}$ is coordinate k of the displacement η_i:

$$\sum_i (\eta_{i,k} p_{i,l} - \eta_{i,l} p_{i,k}) = 0 \quad (k, l \in \{1,2,3\}). \tag{2}$$

These equations make the displacement orthogonal to infinitesimal rotations. Each displacement also has the radial component $\langle p_i, \eta_i \rangle = -\|\eta_i\|^2/2$, by the exact unit-sphere identity. Thus the displacement itself need not lie in the tangent plane.

2.3.2 Stationarity and the full second variation

We establish stationarity and a positive quadratic bound for every perturbation after removing infinitesimal rotations. The candidate is stationary with respect to arbitrary tangent motions of all ten points. Write ∇_i for the gradient with respect to the three coordinates of point i. Since the energy is invariant under orthogonal maps and relabeling, its gradient transforms under the candidate's symmetries in the same way as the points do. A quarter-turn fixes each pole, so its gradient is vertical. The reflection in the vertical plane through p_2 fixes p_2, so its gradient lies in that plane. After removing the radial direction, the only possible gradient component there is along the motion of p_2 as the height changes.

All eight square points form one orbit under the fixed D_{4d} group, and changing height respects these same symmetries. Their contributions to the height derivative are therefore equal; the poles do not move. Thus $S(h_*)$ is eight times the contribution of p_2. Its vanishing makes that tangential component zero, and symmetry does the same at all eight square points. Every gradient is consequently radial.

More precisely, $\nabla_i \mathcal{E}(p) = \lambda_i p_i$, where $\lambda_i = -\frac{1}{2} \sum_{j \ne i} \|p_i - p_j\|^{-1}$. We call λ_i the radial coefficient; it is the spherical Lagrange multiplier.

Let $H(h)$ be the 30×30 matrix at $p(h)$ defined by the following blocks, and abbreviate $H = H(h_*)$. At the stationary candidate it is the constrained second variation. In the block formula at a general height, the radial coefficient means $\lambda_i(h) = -\frac{1}{2} \sum_{j \ne i} \|p_i(h) - p_j(h)\|^{-1}$; stationarity is

asserted only at h_*. For a nonzero pair-difference vector d, the pair Hessian is

$$B(d) = \frac{3dd^{\mathsf{T}}}{\|d\|^5} - \frac{I_3}{\|d\|^3},$$

where the off-diagonal block of H for two different point indices is the negative of $B(p_i - p_j)$. The diagonal block at point i is the sum of $B(p_i - p_j)$ over the other nine points, minus the radial coefficient at that point times the three-by-three identity. These blocks specify the sphere-constrained second variation, including the radial correction.

Similarly, let $R(h)$ have as its three columns the standard coordinate-axis infinitesimal rotations of $p(h)$, each with unit angular speed, and abbreviate $R = R(h_*)$.

Matrix bound. The exact matrix bound is

$$H + RR^{\mathsf{T}} - \frac{1}{20} I_{30} \succeq 0. \tag{3}$$

Rational interval arithmetic verifies the same inequality with $H(h)$ and $R(h)$ throughout $[a, b]$, hence at h_*. An invertible change of basis, applied by congruence to the matrix on the left of (3), transforms it into one with strictly positive diagonal entries, each greater than the sum of the absolute values of the other entries in its row. This strict diagonal dominance proves positive definiteness; the inverse change of basis gives (3). Appendix D.5 gives the matrix calculation. For the concatenated displacement η, equation (2) gives $R^{\mathsf{T}}\eta = 0$, and (3) implies $\eta^{\mathsf{T}} H \eta \geq \rho^2/20$. The alignment allows all orthogonal maps; R removes their continuous rotation directions. The estimate covers every nearby point of $(S^2)^{10}$ after orthogonal alignment, including perturbations that break D_{4d} symmetry.

2.4 Proof of Theorem 1

Section 2.1 and Appendix A establish the candidate. Lemma 1, the checked classification (1) and alignment reduce competitors of no greater energy to the local estimate. Since $10^{-6} \leq 1/1000$, its radius hypothesis is satisfied. We use (3) and the following remainder bound.

Proof of Theorem 1. For a nonzero pair-difference vector d and its perturbation w, put $\ell = \|d\| > 0$.

Pair remainder bound. For $\|w\| \leq \ell/200$, the algebraic pair estimate is

$$\frac{1}{\|d + w\|} \geq \frac{1}{\ell} - \frac{\langle d, w\rangle}{\ell^3} + \frac{3\langle d, w\rangle^2 - \ell^2\|w\|^2}{2\ell^5} - \frac{51}{50}\frac{\|w\|^3}{\ell^4}. \tag{4}$$

The summed remainder estimate is given in Appendix C. The linear terms also have a quadratic expression on the sphere. By radial stationarity, their sum is the sum, over points, of the radial coefficient times $\langle p_i, \eta_i\rangle$. The exact sphere identity $\langle p_i, \eta_i\rangle = -\|\eta_i\|^2/2$ makes this minus one half of the sum of the radial coefficients times the squared displacements. Adding the quadratic terms from the pair Hessians therefore gives one half of the constrained quadratic form $\eta^{\mathsf{T}} H \eta$: the radial correction is exactly the one subtracted in the diagonal blocks of H. Consequently, throughout $\rho \leq 1/1000$, one obtains

$$\mathcal{E}(y) - \mathcal{E}(p) \;\geq\; \frac{1}{2}\eta^{\mathsf{T}} H \eta - \frac{153}{10}\rho^3 \;\geq\; \frac{\rho^2}{40} - \frac{153}{10}\rho^3 \;\geq\; \frac{\rho^2}{200}.$$

For every nonzero aligned displacement with $\rho \leq 1/1000$, the final quantity is positive. Since $\mathcal{E}(y) = \mathcal{E}(x) \leq \mathcal{E}(p)$, the inequality forces $\rho = 0$, hence $y = p$ exactly. Every competitor of energy at most $\mathcal{E}(p)$ is therefore congruent to p; all remaining competitors have strictly larger energy. Conversely, orthogonal transformations and permutations preserve energy. This proves both optimality and the equality case in Theorem 1. The candidate itself attains the minimum. □

3 Formal verification

Theorem 1 and its proof are formalized in Lean. The theorem `ThomsonN10.thomson_ten_complete` states:

> Exactly one real height $h \in [a, b]$ satisfies $S(h) = 0$. For every such height and every injective map $x : \{0, \ldots, 9\} \to S^2$, $\mathcal{E}(p(h)) \leq \mathcal{E}(x)$, with equality if and only if x is congruent to $p(h)$.

The interval, stationarity equation and candidate coordinates are the ones defined above. The formal hypotheses are unit norm and injectivity; the energy is the same unordered-pair sum, and orthogonal congruence includes reflections. The candidate's unit norms and distinctness are also proved in Lean. The checking notes give the definitions and standard logical axioms, and distinguish the supplementary numerical illustrations from the formal proof.

Appendix A Candidate energy and interval data

We verify admissibility and evaluate the candidate energy. The candidate is admissible: in the coordinates above, unit norm follows from $r^2 = 1 - h_*^2$ and $2q^2 = r^2$. The two poles and the two squares have distinct heights; within each square the four planar coordinates are distinct because $r, q > 0$. Thus the ten points are distinct.

The 45 unordered pairs consist of one pole pair, eight neighboring and four opposite pairs within the squares, two classes of eight pairs between the squares, and sixteen pole–square pairs. Grouping them gives

$$F(h) = \frac{1}{2} + \frac{4\sqrt{2}+2}{\sqrt{1-h^2}} + \frac{8}{\sqrt{2-\sqrt{2}+(2+\sqrt{2})h^2}} + \frac{8}{\sqrt{2+\sqrt{2}+(2-\sqrt{2})h^2}} + \frac{8}{\sqrt{2-2h}} + \frac{8}{\sqrt{2+2h}}. \tag{5}$$

The terms appear in that order: pole pair, pairs within the squares, the two between-square classes, and the two pole–square classes. Write $S(h) = F'(h)$ for the derivative of this energy with respect to height. Its explicit formula is given in Appendix D.1. Let $[a, b]$ be the exact rational interval defined in Appendix D.1. It satisfies $0 < a < b < 1$ and $b - a = 1/(2D) < 2^{-300}$, where the integer denominator D is given there. For orientation, this narrow interval lies inside

$$[0.42268742404398, 0.42268742404400].$$

Its decimal begins $0.422687424043986\ldots$. The root existence and uniqueness in this interval are proved in Lean.

Appendix B Finite classification of interval assignments

The table records the candidate's distance classes. An anchor triple must exist. For example, the candidate's pole pair receives the color of the window centered at -1. The nine witnesses correspond to nine enumerated node subsets with their anchor types; all give the same candidate pattern up to relabeling.

Color	Candidate inner product	Number of pairs
0	-1	1
1	h_*	8
2	$-h_*$	8
3	h_*^2	8
4	$2h_*^2 - 1$	4
5	$(1 - h_*^2)/\sqrt{2} - h_*^2$	8
6	$-(1 - h_*^2)/\sqrt{2} - h_*^2$	8

The subsequent enumeration treats all 43 eligible anchor types. Reorder the three anchor points so that the colors of their pairs (first, second), (first, third), (second, third) are nondecreasing. Permuting three vertices permits every permutation of their three edges, so such an order always exists. The node coordinates in Section 2.2 use this fixed order. For example, the candidate triple p_2, p_3, p_6 has ordered pair colors $(3, 5, 5)$.

The classification is proved in Lean; the checking notes identify its certificate and formal soundness statement.

Appendix C Remainder estimates

The following estimates supply the pair bounds used in Section 2.4.

C.1 Pair remainder and summed error

For this second-order Taylor bound with cubic error, put $z = (2\langle d, w\rangle + \|w\|^2)/\ell^2$. The proof bounds $(1+z)^{-1/2}$ below by $1 - z/2 + 3z^2/8 - 5z^3/16$ on $-1 < z \le 1$, then applies this bound to the normalized pair displacement. Every candidate pair distance is at least one. For $d = p_i - p_j$, $w = \eta_i - \eta_j$, the geometric bounds are

$$\|\eta_i - \eta_j\| \le \tfrac{3}{2}\rho, \qquad \sum_{i<j} \|\eta_i - \eta_j\|^3 \le 15\rho^3.$$

The first follows from $\|\eta_i - \eta_j\| \le \sqrt{2}\rho \le \frac{3}{2}\rho$. For the second, the identity for the sum of squared pair differences gives $\sum_{i<j} \|\eta_i - \eta_j\|^2 \le 10\rho^2$. Multiplying this by the largest pair displacement gives the cubic bound. For $\rho \le 1/1000$, these satisfy the hypothesis of (4). Summing the error over all 45 pairs bounds it by $(51/50)15\rho^3 = (153/10)\rho^3$.

Appendix D Certificate data

The following data give the rational bounds used in the proof.

D.1 The exact height interval

We define the rational interval and stationarity equation. For the rational height interval used in Section 1, let A and D be the integers defined below, with D the denominator. Its endpoints a, b are defined by

$$a = A/D, \qquad b = (2A+1)/(2D),$$

$A = 513213568640798381215999065069135718731748351905698829816800875926548421101580455514066781,$
$D = 2^{283} \cdot 5^7.$

For the explicit stationarity equation, set

$$u_-(h) = 2 - \sqrt{2} + (2+\sqrt{2})h^2, \qquad u_+(h) = 2 + \sqrt{2} + (2-\sqrt{2})h^2.$$

The derivative of the family energy is

$$S(h) = \frac{(4\sqrt{2}+2)h}{(1-h^2)\sqrt{1-h^2}} - \frac{8(2+\sqrt{2})h}{u_-(h)\sqrt{u_-(h)}} - \frac{8(2-\sqrt{2})h}{u_+(h)\sqrt{u_+(h)}} + \frac{8}{(2-2h)\sqrt{2-2h}} - \frac{8}{(2+2h)\sqrt{2+2h}} = F'(h). \tag{6}$$

D.2 The separation polynomial

Separation of points. Rational interval evaluation gives $\mathcal{E}(p) \le 32717/1000$ (Appendix D.4), so this is also an energy cap for the competitor. Let g be the quartic polynomial defined below. It lies below f on the whole interval $[-1, 1)$ and has nonnegative coefficients in the Legendre basis. The spherical-harmonic addition identity therefore expresses the sum of $g(\langle x_i, x_j\rangle)$ over

all ordered pairs, including the diagonal, as a constant plus nonnegative weighted squares. Each square is the square of the sum, over the ten points, of a fixed spherical harmonic of degree one through four. Subtracting the diagonal contribution and dividing by two gives a lower bound of $13111005315721/401353681050 > 32.666$ for the sum over unordered distinct pairs. If any pair had inner product at least $13/20$, its energy minus g would exceed $51/1000$. All other pair differences are nonnegative. Adding $51/1000$ to the exact polynomial lower bound exceeds $32717/1000$ by more than 0.00096, a contradiction. Thus $\langle x_i, x_j\rangle < 13/20$ for every $i \neq j$.

This records the quartic used to exclude too-close pairs before applying the three-point bound. Write P_k for the Legendre polynomial of degree k, normalized by $P_k(1) = 1$. The polynomial is

$$g(t) = \frac{17\,366\,680\,031}{21\,123\,877\,950} + \frac{833\,419\,493\,024}{1\,672\,307\,004\,375}P_1(t) + \frac{1\,760\,733\,078\,976}{7\,023\,689\,418\,375}P_2(t) + \frac{17\,766\,191\,104}{185\,811\,889\,375}P_3(t) + \frac{5\,504\,237\,568}{260\,136\,645\,125}P_4(t).$$

The nonnegative coefficients give the spherical-harmonic sum identity. The inequalities $g(t) \le f(t)$ on $[-1, 1)$ and $f(t) - g(t) > 51/1000$ on $[13/20, 1)$ follow from exact polynomial identities with nonnegative Bernstein coefficients.

D.3 The three-point kernel polynomials

The kernel K has a nonnegative sum over triples, as follows.

For block k, let $J^{(k)}$ be its supplied factor matrix (the integer entries divided by 2^{200}, with unused entries set to zero in an eleven-by-eleven matrix). Its column polynomials and the polynomial with this distinguished first point are

$$\phi_{kr}(u) = \sum_{i=0}^{10} J^{(k)}_{ir} u^i, \qquad \mathcal{A}_k(u, v, t) = \sum_{r=0}^{10} \phi_{kr}(u)\phi_{kr}(v)T_k(u, v, t).$$

Let $\overline{\mathcal{A}}_k$ be the average of $\mathcal{A}_k$ over all six permutations of its three arguments. The repeated-index correction and full kernel are

$$K_k(u, v, t) = 8\overline{\mathcal{A}}_k(u, v, t) + \overline{\mathcal{A}}_k(u, u, 1) + \overline{\mathcal{A}}_k(v, v, 1) + \overline{\mathcal{A}}_k(t, t, 1) + \tfrac{1}{9}\overline{\mathcal{A}}_k(1, 1, 1),$$
$$K(u, v, t) = \sum_{k=0}^{9} K_k(u, v, t).$$

The coefficients account for repeated indices in the full triple sum. There are $10 \cdot 9 \cdot 8 = 720$ ordered triples with distinct indices, $10 \cdot 9 = 90$ for each of the three ways exactly two indices coincide, and ten with all indices equal. Divide the full sum by 90: the distinct triple average has coefficient $720/90 = 8$, each repeated-pair average has coefficient one, and the constant has coefficient $10/90 = 1/9$. Averaging K_k over distinct triples gives exactly this normalized full sum. Its nonnegativity therefore gives the required distinct-triple positivity of K.

D.4 The three-point certificate

We record the exact certificate bounds. Interval evaluation of the candidate gives $\mathcal{E}(p) \le U$, where $U \approx 32.716949460147588154557057519699 94$. Its exact value is given below.

The sum $\|\mathcal{R}\|_1$ of the absolute values of the residual's rational coefficients is tiny: $\|\mathcal{R}\|_1 \approx 1.1673222012517146 \cdot 10^{-56}$.

Put $L = 45(2^{-130} + \|\mathcal{R}\|_1)$; numerically, $L \approx 3.306077861687684 \cdot 10^{-38} < 10^{-30}$. Averaging the defining identity over distinct triples and using the two positivity properties gives Lemma 1.

The candidate inequality in Lemma 1 is the separately established interval bound above. For the pair-sum inequality, the unit-vector hypotheses put every triple in the Gram domain, while the pair cap gives $u, v, t \le 13/20$, where all weights of W are nonnegative. The triple-to-pair averaging in Section 2.2 explains the factor 45 in L. The much weaker separation bound used Delsarte–Yudin linear programming [5, Section 1] [6, Section 1.1]; here the error is small enough to force every pair into a candidate window.

The following rational data and weights give Lemma 1. The polynomial coefficients are the fixed rational data in the certificate `data/certificate.json.gz` of the published development (linked below the title). Its candidate-energy bound is the exact rational

$$U = \frac{52\,574\,110\,779\,609\,793\,015\,977\,559\,478\,279\,245\,057\,879\,406\,410\,836\,764\,596\,571\,436}{2^{200}}.$$

Write $\Delta = 1 + 2uvt - u^2 - v^2 - t^2$ for the Gram determinant. Before averaging over permutations of u, v, t, the six weights multiplying polynomial squares are 1, $1+u$, $13/20-u$, Δ, $(1+u)(13/20-u)$ and $\Delta(1+u)(13/20-u)$. Each is used for two blocks, one symmetric and one antisymmetric under interchange of v, t; after squaring and permutation averaging all twelve blocks are nonnegative on the same Gram domain.

Scalar inequalities. The minorant and the slack bound outside the windows are certified by subdividing rational intervals and checking nonnegative Bernstein coefficients of integer polynomials. The substitution $t = 1 - 2y^2$, with $y = \sqrt{(1-t)/2} > 0$, turns the reciprocal-square-root inequalities into polynomial inequalities after multiplication by positive denominators.

D.5 Interval matrix verification

The interval Hessian calculation encloses the arithmetic and square-root operations over the full height interval. Its change-of-basis matrix is upper triangular with all diagonal entries equal to one, hence invertible. Interval bounds on the transformed matrix certify strict diagonal dominance.

References

[1] J. J. Thomson, On the structure of the atom: an investigation of the stability and periods of oscillation of a number of corpuscles arranged at equal intervals around the circumference of a circle; with application of the results to the theory of atomic structure, *Philosophical Magazine* 7 (1904), 237–265. doi:10.1080/14786440409463107.

[2] A. Karthigeyan, *The Nine-Point Coulomb Thomson Problem*, Lean project (2026). Repository.

[3] P. Delsarte, J. M. Goethals and J. J. Seidel, Spherical codes and designs, *Geometriae Dedicata* 6 (1977), 363–388. doi:10.1007/BF03187604.

[4] V. A. Yudin, Minimum potential energy of a point system of charges, *Diskretnaya Matematika* 4 (1992), no. 2, 115–121; English translation in *Discrete Mathematics and Applications* 3 (1993), no. 1, 75–81. doi:10.1515/dma.1993.3.1.75.

[5] C. Bachoc and F. Vallentin, New upper bounds for kissing numbers from semidefinite programming, *Journal of the American Mathematical Society* 21 (2008), 909–924. doi:10.1090/S0894-0347-07-00589-9.

arXiv:math/0608426.

[6] H. Cohn and J. Woo, Three-point bounds for energy minimization, *Journal of the American Mathematical Society* 25 (2012), 929–958. arXiv:1103.0485.

[7] L. Föppl, Stabile Anordnungen von Elektronen im Atom, in *Proceedings of the Fifth International Congress of Mathematicians*, Cambridge, 1912, vol. II (Cambridge University Press, 1913), 188–191. `https://www.mathunion.org/fileadmin/ICM/Proceedings/ICM1912.2/ICM1912.2.ocr.pdf`.

[8] N. N. Andreev, An extremal property of the icosahedron, *East Journal on Approximations* 2 (1996), no. 4, 459–462.

[9] H. Cohn and A. Kumar, Universally optimal distribution of points on spheres, *Journal of the American Mathematical Society* 20 (2007), 99–148. arXiv:math/0607446.

[10] R. E. Schwartz, The 5 Electron Case of Thomson's Problem (2010). arXiv:1001.3702.

[11] T. Erber and G. M. Hockney, Equilibrium configurations of N equal charges on a sphere, *Journal of Physics A: Mathematical and General* 24 (1991), L1369–L1377, Table 1. doi:10.1088/0305-4470/24/23/008. `https://lss.fnal.gov/archive/1991/pub/Pub-91-222-T.pdf`.

[12] D. J. Wales and S. Ulker, Cambridge Cluster Database, Thomson problem, ten-point entry. `https://www-wales.ch.cam.ac.uk/~wales/CCD/Thomson/table.html`.

[13] `saberwatchmanga` (formerly `terry2418`), *Lean Certificates: Finite Results and Thomson N=10*. Lean project (2026). Repository.

[14] H. Tran, A Lean Proof of the Thomson Problem for Seven Electrons, Vals AI blog (2026). `https://www.vals.ai/blogs/thomson-n7-lean-proof`.

[15] L. Kryvonos, L. Liehr and M. A. Taylor, Energy minimization for eight points on the sphere (2026). arXiv:2609.22077.

[16] J. Tooby-Smith and A. Zughaid, A warrant for the N = 8 Thomson problem, in Lean 4, Lean project (2026). Repository.

[17] A. Zarco (`alejandrozarco`), *Five points on the sphere: exact three-point certificates for the Riesz energies $s = 1, \dots, 6$, and Lean formalisations for $s = 1$ (Coulomb) and $s = 2$*, `five-points-riesz`, Lean project (2026). Repository.

[18] A. Zarco (`alejandrozarco`), *The pentagonal bipyramid as the unique logarithmic-energy minimiser for seven points on the sphere: an unreviewed Lean 4 warrant (Conjecture 1 of Armentano et al.)*, `thomson-n7-log`, Lean project (2026). Repository.

[19] `saberwatchmanga` (formerly `terry2418`), *Lean-verified local minimality for ten charges on a sphere*, `Thomson10LocalMinimum`, Lean project (2026). Repository.

[20] `saberwatchmanga` (formerly `terry2418`), *A Lean-checked distance restriction for ten charges on a sphere*, `Thomson10Chord1935`, Lean project (2026). Repository.

[21] P. Graham, *The Thomson problem for $N = 10$*, proof sources and certificates (2026). Repository.

[22] K. Xie, *Optimality and uniqueness for the Thomson problems with $n = 9$ and $n = 10$*, preprint, Zenodo, version 1.0.0, November 2, 2026. doi:10.5281/zenodo.23899872; ten-point verification code and certificates, doi:10.5281/zenodo.23845064. The proof uses three-point energy bounds, Gram classification and a Hessian bound with exact and interval arithmetic.

[23] P. Graham, *The Thomson problem for $N = 10$*, version 1, first public release, October 22, 2026: repository tag `thomson-10-v1` (commit `bc8bd8c`).

[24] Jingxing Huang (`Stickerbug`), *Thomson n=9 formal proof and manuscript*, `thomson-n9-proof`, archived release (2026). doi:10.5281/zenodo.23573471; repository revision of October 25, 2026, README and *A Lean-Verified Computer-Assisted Proof of the Nine-Point Thomson Minimum*, abstract.